Osaka Feedback Model II: Modeling Supernova Feedback Based on High-Resolution Simulations

Yuri Oku[1] , Kengo Tomida[2], Kentaro Nagamine[1,3,4] ,
Ikkoh Shimizu[5] and Renyue Cen[1,6]

[1]Theoretical Astrophysics, Department of Earth & Space Science, Graduate School of Science, Osaka University, 1-1 Machikaneyama, Toyonaka, Osaka 560-0043, Japan
email: oku@astro-osaka.jp

[2]Astronomical Institute, Tohoku University, Aoba, Sendai, Miyagi 980-8578, Japan

[3]Kavli IPMU (WPI), The University of Tokyo, 5-1-5 Kashiwanoha, Kashiwa, Chiba 277-8583, Japan

[4]Department of Physics & Astronomy, University of Nevada, Las Vegas, 4505 S. Maryland Pkwy, Las Vegas, NV 89154-4002, USA

[5]Shikoku Gakuin University, 3-2-1 Bunkyocho, Zentsuji, Kagawa, 765-8505, Japan

[6]Department of Astrophysical Sciences, Princeton University, Peyton Hall, Princeton, NJ 08544, USA

Abstract. Feedback from supernovae (SNe) is an essential mechanism that self-regulates the growth of galaxies. We build an SN feedback model based on high-resolution simulations of superbubble and SN-driven outflows for the physical understanding of the galaxyCGM connection. Using an Eulerian hydrodynamic code `Athena++`, we find universal scaling relations for the time evolution of superbubble momentum, when the momentum and time are scaled by those at the shell-formation time. We then develop an SN feedback model utilizing Voronoi tessellation, and implement it into the `GADGET3-Osaka` smoothed particle hydrodynamic code. We show that our stochastic thermal feedback model produces galactic outflow that carries the metals high above the galactic plane but with weak suppression of star formation. Additional mechanical feedback further suppresses star formation. Therefore, we argue that both thermal and mechanical feedback is necessary for the SN feedback model of galaxy evolution when an individual SN bubble is unresolved.

Keywords. Galaxy formation, Numerical simulation, Stellar feedback, Supernovae, Galactic winds

1. Introduction

Supernova feedback (SN FB) is an essential mechanism that self-regulates the growth of galaxies, and a better understanding of SN FB is necessary to resolve the rise and fall of star formation in galaxies. Numerical simulations are a powerful tool to study the nonlinear evolution of galaxies on a cosmological timescale. However, it is challenging to resolve individual SN bubbles in galaxy simulations due to their low resolution of mass and space, which are not enough to resolve the cooling mass and length of the SN bubble. Therefore, it is necessary to model the effect of SN FB on sub-resolution scale, and many flavors of SN FB subgrid models have been developed (e.g., Stinson et al. 2006; Dalla Vecchia & Schaye 2012; Keller et al. 2014; Kimm & Cen 2014; Hopkins et al. 2018).
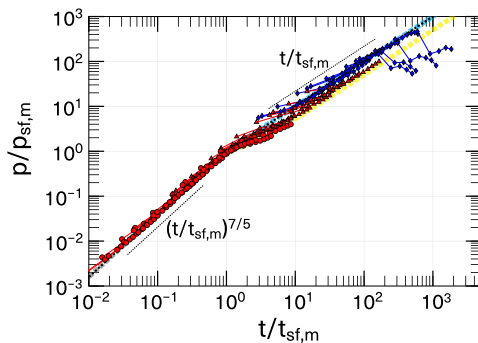
Figure 1. Evolution of momentum p normalized by $p_{\rm sf,m}$ vs. time t normalized by $t_{\rm sf,m}$. Red and blue points depict the runs with $\Delta t_{\rm SN} < 0.1 t_{\rm PDS}$ and $\Delta t_{\rm SN} > 0.1 t_{\rm PDS}$, respectively. Different symbols connected by lines correspond to runs at different SN intervals: $\Delta t_{\rm SN} = 0.01$ Myr (circle), $\Delta t_{\rm SN} = 0.1$ Myr (triangle), $\Delta t_{\rm SN} = 1$ Myr (diamond). The black dotted lines indicate the $(p/p_{\rm sf,m}) \propto (t/t_{\rm sf,m})^{7/5}$ and $(p/p_{\rm sf,m}) \propto (t/t_{\rm sf,m})$ power law, respectively.

In this work, we focus on two effects of SN FB: mechanical FB driving interstellar turbulence and thermal FB launching hot outflows. We show that models are necessary for both FB modes; mechanical FB model for spatially unresolved growth of superbubble, and stochastic thermal FB model for hot gas unresolved in mass. For the mechanical FB, we first investigate the momentum input by superbubble using an Eulerian hydrodynamic code Athena++ and derive a formula to predict the input momentum for given density and metallicity of the interstellar medium (ISM).

This article is based on our published paper (Oku et al. 2022), and the interested readers are referred to the paper for further details.

2. Athena++ simulation of superbubbles

We perform a suite of three-dimensional hydrodynamical simulations of a superbubble using Athena++ (Stone et al. 2020). The SN energy of 10^{51} erg is injected ten times with a fixed time interval $\Delta t_{\rm SN}$ at the center of the simulation box. We investigate the dependence of the momentum of a superbubble on the density n and metallicity Z of the ISM and $\Delta t_{\rm SN}$. The parameter ranges investigated in this work are $n/{\rm cm}^{-3} \in \{0.1, 1, 10\}$, $Z/Z_\odot \in \{10^{-3}, 10^{-2}, 10^{-1}, 1\}$, and $\Delta t_{\rm SN}/{\rm Myr} \in \{0.01, 0.1, 1\}$, and the simulation suite consists of 36 simulations with different combinations of n, Z, and $\Delta t_{\rm SN}$. The size of the simulation box is $L/{\rm pc} = 135,\ 300,\ 900$ for cases of $n/{\rm cm}^{-3} = 0.1,\ 1,\ 10$, and the simulation box has periodic boundaries.

Figure 1 shows the time evolution of the momentum of the simulated superbubbles with x- and y-axis normalized by the time and momentum at the shell formation. We extend the analytic estimation of the shell formation time $t_{\rm sf,m}$ by Kim & Ostriker (2015) and Kim et al. (2017) by including the metallicity dependence:

$$t_{\rm sf,m} = 1.7 \times 10^4\ {\rm yr}\ E_{51}^{0.28}\ \Delta t_{\rm SN,6}^{-0.28}\ n_0^{-0.71}\ \Lambda_{6,-22}^{-0.42}, \tag{2.1}$$

where $E_{51} = E_{\rm SN}/10^{51}$ erg, $\Delta t_{\rm SN,6} = \Delta t_{\rm SN}/1$ Myr, $n_0 = n/1\,{\rm cm}^{-3}$, and $\Lambda_{6,-22} = \max(1.9 - 0.85\,Z/Z_\odot, 1.05)\,(Z/Z_\odot) + 10^{-1.33}$. Here, $\Lambda_{6,-22}$ is the fitting function to the value at $T = 10^6$ K of the metal cooling function by Sutherland & Dopita (1993).

The normalized time evolution of the superbubble momentum show universality over a wide range of environments, indicating that the shell-formation time is the characteristic timescale of superbubble growth, which is consitent with the previous finding by Kim et al. (2017).
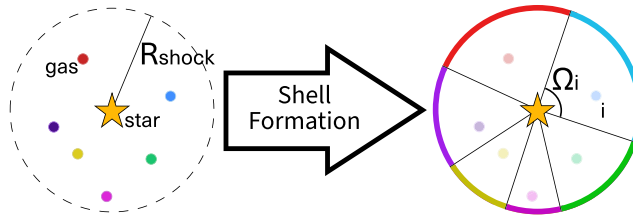
Figure 2. Schematic description of the spherical superbubble feedback model developed in this work. The left-hand side shows the particle distribution of gas and star particles when the supernova explosion takes place, whereas the right-hand side shows the superbubble shell formation, and how we split the shell using Voronoi tessellation based on the gas particle distribution inside the bubble.

We further derive the momentum of superbubble per SN assuming the initial star cluster mass function $dN/dM \propto M^{-2}$ (Krumholz et al. 2019):

$$\hat{p} = 1.75 \times 10^5 \, M_\odot \, \mathrm{km \, s^{-1}} n_0^{-0.05} \, \Lambda_{6,-22}^{-0.17}. \tag{2.2}$$

The dependency on $\Lambda_{6,-22}$ indicates that the momentum input by superbubble is larger by a factor of three in a zero metallicity environment than in solar metallicity.

3. Construction of SN FB model

In this section, we construct an SN FB model for particle-based simulations of galaxy formation.

Mechanical FB Model. We model the mechanical effect of SN FB using Equation (2.2) to predict the amount of momentum input by SNe at the SN event site. We distribute the momentum input to surrounding gas particles using Voronoi tesselation as illustrated in Figure 2. The surrounding particles are projected to the surface of a sphere centered at the SN site, and the Voronoi tesselation is performed on the surface. We use the solid angle to the face on the Voronoi polyhedron Ω_i for weighting the SN input to the surrounding particles.

Stochastic Thermal FB Model. Superbubbles can grow to the size of galactic disk scale height, and then break out to produce energetic outflow (Fielding et al. 2018). We model this wind launching effect by SNe as stochastic thermal energy injection, similar to the model developed by Dalla Vecchia & Schaye (2012). We use the entropy $S = k_B T n^{1-\gamma}$ as a controlling parameter. Hu (2019) showed that typical entropy of hot outflow to be $10^8 - 10^9 \, k_B \, \mathrm{K \, cm^2}$ using a high-resolution dwarf galaxy simulation, and we adopt $S_{FB} = 10^8 \, k_B \, \mathrm{K \, cm^2}$ as the default value. We stochastically inject thermal energy ΔE_i to increase the entropy of a i-th particle to S_{FB}, and the probability of injecting thermal energy to i-th particle is $P_i = \Delta E_i / (\Omega_i E_{FB,th})$, where $E_{FB,th}$ denotes the total thermal energy input by the SN event, which is set to 70% of total energy input.

4. `GADGET3-Osaka` simulation of isolated galaxies

To explore the thermal and mechanical FB effects, we run five simulations with different FB settings summarized in Table 1. We implement the FB model described in the previous section to the smoothed particle hydrodynamics code `GADGET3-Osaka` (Shimizu et al. 2019) which includes radiative cooling, heating, and star formation models as described in Oku et al. (2022). The initial condition is an isolated Milky-way-mass galaxy, taken from the AGORA project (Kim et al. 2014), and we add gas halo following Shin et al. (2021). We evolve the system to 1 Gyr with subgrid physics turned on after evolving it adiabatically to 0.5 Gyr for relaxation. In the following, we show the time evolution of the simulated galaxies for 1 Gyr with subgrid physics.

Table 1. List of isolated galaxy simulations used in this work

Run Name	FB Type				Notes
	SNII-M[a]	SNII-T[b]	Stochastic[c]	SNIA & OB[d]	
Fiducial	✓	✓	✓	✓	Fiducial run with all feedback models
Non-stochastic	✓	✓		✓	Fiducial but thermal energy is distributed without stochastic treatment
SNII-kinetic	✓				Type II SN mechanical feedback only
SNII-thermal		✓	✓		Type II SN thermal feedback only
No-FB					No feedback

Notes. Model description of simulations used in this work. The leftmost column shows the name of run, the rightmost column shows notes, and the middle four columns show FB types activated in the simulation.
[a]Type-II SN mechanical FB
[b]Type-II SN thermal FB
[c]Stochastic thermal FB
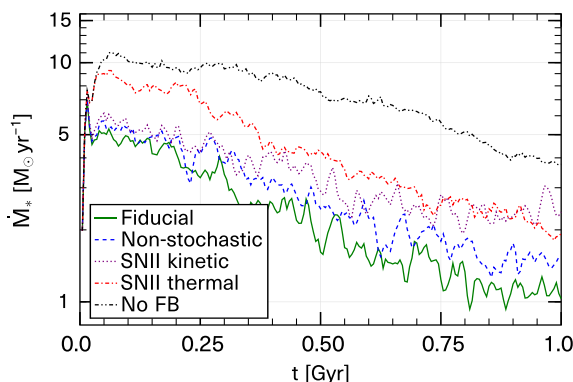[d]Type-Ia and OB star mechanical FB

Figure 3. Star formation rate as a function of time for the isolated galaxy simulations given in Table 1. The No-FB run has the highest SFR, and the SNII-thermal run shows weak suppression of SFR. In other runs, SFR is suppressed by the mechanical SN FB efficiently.
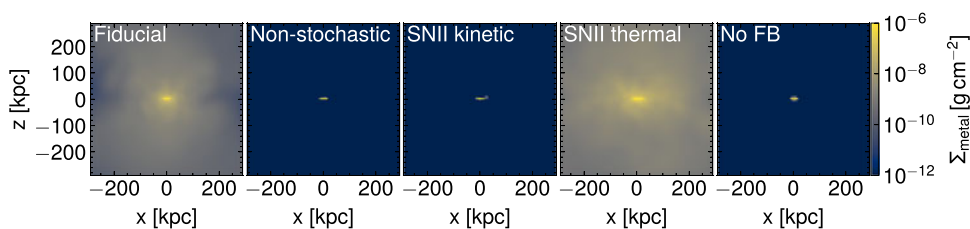

Figure 4. Edge-on view of metal column density at $t \simeq 1$ Gyr. It is clear that the metals are carried over large distances in the Fiducial and SNII-thermal runs.

Figure 3 shows the history of star formation rates of simulated galaxies. Three runs with Type II SN mechanical FB, Fiducial, Non-stochastic, and SNII-Kinetic runs, show strongly suppressed star formation while SNII-Thermal run shows weaker suppression. The Fiducial and Non-stochastic runs show similar star formation history, indicating that the stochastic thermal feedback has a minor effect on the suppression of star formation, while the Fiducial run shows a slightly lower star formation rate.

Figure 4 shows the edge-on view of metal column density of simulated galaxies at $t \simeq 1$ Gyr. One can clearly see that metals are carried over large distances in the Fiducial and SNII-Thermal runs, indicating strong outflow is produced by stochastic thermal FB as intended in our modeling.

5. Conclusion and Future Prospects

We have studied the environment dependence of the momentum input from superbubble by three-dimensional hydrodynamical simulation using `Athena++` code, and obtained Equation (2.2), which predicts the momentum input per SN for given density and metallicity of ISM. We then constructed the SN FB model for particle-based simulation using Voronoi tessellation as shown in Figure 2. We separately modeled the mechanical and thermal effect of SN FB based on results from high-resolution simulations. We have implemented the SN FB model into `GADGET3-Osaka` code, and performed isolated milky-way-mass galaxy simulations. We have demonstrated that the mechanical FB suppresses star formation while stochastic thermal FB drives strong metal outflows.

We have performed idealized isolated galaxy simulations in this work, and more realistic cosmological simulation is necessary to compare our result to observational data. We will investigate metal distribution in CGM and statistics of galaxies, e.g., galaxy stellar mass function and mass-metallicity relation, in cosmological simulations with our SN FB model developed in this work, and compare them with observations in our future work.

References

Dalla Vecchia, C. & Schaye, J. 2012, *MNRAS*, 426, 140
Fielding, D., Quataert, E., & Martizzi, D. 2018, *MNRAS*, 481, 3325
Hopkins, P. F., Wetzel, A., Kereš, D., *et al.* 2018, *MNRAS*, 477, 1578
Hu, C.-Y. 2019, *MNRAS*, 483, 3363
Keller, B. W., Wadsley, J., Benincasa, S. M., & Couchman, H. M. P. 2014, *MNRAS*, 442, 3013
Kim, J.-H., Abel, T., Agertz, O., *et al.* 2014, *ApJS*, 210, 14
Kim, C.-G. & Ostriker, E. C. 2015, *ApJ*, 802, 99
Kim, C.-G., Ostriker, E. C., & Raileanu, R. 2017, *ApJ*, 834, 25
Kimm, T. & Cen, R. 2014, *ApJ*, 788, 121
Krumholz, M. R., McKee, C. F., & Bland-Hawthorn, J. 2019, *ARAA*, 57, 227
Oku, Y., Tomida, K., Nagamine, K., Shimizu, I., & Cen, R. 2022, *ApJS*, 262, 9
Shimizu, I., Todoroki, K., Yajima, H., & Nagamine, K. 2019, *MNRAS*, 484, 2632
Shin, E.-J., Kim, J.-H., & Oh, B. K. 2021, *ApJ*, 917, 12
Stinson, G., Seth, A., Katz, N., Wadsley, J., Governato, F., & Quinn, T. 2006, *MNRAS*, 373, 1074
Stone, J. M., Tomida, K., White, C. J., & Felker, K. G. 2020, *ApJS*, 249, 4
Sutherland, R. S. & Dopita, M. A. 1993, *ApJS*, 88, 253